

ma cells, one would expect an increase in the number of cells with the  $G_0$ - $G_1$  complement of DNA. Although Maden does not report controls for nerve dependence similar to those in our experiment, we suspect that the cone stage blastemas in his experiment were nerve-independent. As figure 2 shows there is no discernible change from the innervated limbs in the overall pattern of the microdensitometric curve following denervation of 15-day regenerates. These results are consistent with those of Mescher and Tassava who have failed to find any abnormal accumulation of cells in denervated limbs. An important point to be made is that the controls continue to proliferate and exhibit their characteristic curve for DNA amounts. The experimental blastemas of day 15, even though denervated, exhibit a curve essentially identical to the controls. In these limbs, mitosis decreases or stops altogether and the blastema regresses to the level of amputation. The fate of blastema cells during regression remains elusive and there is continuing controversy in the literature over where in the

cell cycle the nerve has its influence. Carlone and Foret<sup>9</sup> have provided in vitro evidence to support the idea of Tassava and Mescher that the cells of a denervated limb block in  $G_2$ . When they added newt brain homogenate to blastemas cultured without nerves, they found a burst of mitotic activity after only 8 h. Since the  $G_2$  phase of the blastemal cell cycle lasts from 4 to 8 h<sup>8,10</sup> this suggests that the cells may have been blocked in  $G_2$ . On the other hand, Globus<sup>11</sup> and Olsen and Tassava<sup>12</sup> have suggested that the neurotrophic effect may be a more general one, facilitating the movement of cells from one phase to another until they complete the total cell cycle. In the absence of nerves, cells would stop at all stages rather than one discrete phase. In addition, as has been previously postulated<sup>2</sup>, the cells may then breakdown and/or be phagocytized, or otherwise leave the limb field since the blastemas of denervated, nerve-dependent limbs regress. In these cases, detection of separate populations of cells in denervated limbs would be impossible by the techniques presently employed.

- 1 M. Singer, Q. Rev. Biol. 27, 169 (1952).
- 2 A. L. Mescher and R. A. Tassava, Devl Biol. 44, 187 (1975).
- 3 R. A. Tassava, L. L. Bennett and G. D. Zitnik, J. exp. Zool. 190, 111 (1974).
- 4 M. Singer and L. J. Craven, J. exp. Zool. 108, 279 (1948).
- 5 O. E. Schotte and E. G. Butler, J. exp. Zool. 87, 279 (1941).
- 6 R. A. Tassava and A. L. Mescher, Differentiation 4, 23 (1968).
- 7 M. Maden, J. Embryol. exp. Morph. 50, 169 (1979).
- 8 R. S. Grillo, Oncology 25, 347 (1971).
- 9 R. L. Carlone and J. E. Foret, J. exp. Zool. 210, 245 (1979).
- 10 H. Wallace and M. Maden, J. Cell Sci. 20, 539 (1976).
- 11 M. Globus, Am. Zool. 18, 855 (1978).
- 12 C. L. Olsen and R. A. Tassava, Midwest Reg. devl Biol. Conf. 1980, abstracts.

## Visualization of DNA in various phages (T4, $\chi$ , T7, $\phi$ 29) by ethidium bromide epi-fluorescent microscopy<sup>1</sup>

T. Kuroiwa, S. Nishibayashi, S. Kawano and T. Suzuki

Department of Cell Biology, National Institute for Basic Biology, Okazaki 444 (Japan), 13 January 1981

**Summary.** DNA-containing areas in various phages (T4,  $\chi$ , T7 and  $\phi$  29) could be observed at the light microscopic level using ethidium bromide epi-fluorescent microscopy. The fluorescent intensity per phage was in linear proportion to the DNA content in each phage.

Williamson and Fennel<sup>2</sup> and James and Jope<sup>3</sup> have succeeded in staining T4 phages with a DNA-specific fluorochrome 4'-diamidino-2-phenylindole (DAPI). However, the DNA-DAPI complex must be excited by only UV-light<sup>2</sup>. On the other hand, DNA-ethidium bromide (EB) complex in cells could be excited by both UV and green light<sup>4</sup>. Green light had a lower fading effect on fluorescence (see results) and a lower lethal effect on organisms than UV<sup>5</sup>.

We succeeded in visualizing  $\phi$  29 phages containing very small amounts of DNA ( $11.5 \times 10^6$  daltons)<sup>6</sup> by use of EB, a new staining solution reducing the fading of fluorescence and epi-fluorescent microscopes equipped with green excitation light.

**Materials and methods.** Stocks of T4,  $\chi$  and T7 phages and *Escherichia coli* K-12 were kindly given by Dr Komeda at the National Institute of Genetics in Mishima, and the  $\phi$  29 phages by Dr Hirokawa at the Sophia University in Tokyo. A drop of suspension containing bacteria or phages at a concentration of  $10^6$ - $10^8$  per ml was put on a glass slide, then a drop of the buffer-NS (20 mM Tris-HCl at pH 7.6, 0.25 M sucrose, 1 mM EDTA, 1 mM  $MgCl_2$ , 0.1 mM  $ZnSO_4$ , 0.1 mM  $CaCl_2$ , 0.8 mM phenylmethylsulfonylfluoride, 0.05%  $\beta$ -mercaptoethanol) or distilled water containing EB at the concentration of 50  $\mu$ g per ml was added, and

they were thoroughly mixed. A cover slip was then placed on the mixture. The materials were stained for 30 min.

In order to study fluorescence decay, under a continuous excitation with UV or green light, the fluorescent intensity emitted from the EB stained *E. coli* was examined at 15-sec intervals for 120 sec by use of a Zeiss-MPM 03-Fluorometer equipped with a high-pressure mercury lamp XB0-100 W, filter combination No. 48 77 11 or No. 48 77 15 and a Neofluor 100/1.30 oil objective. The areas of the individual bacterial nuclei were optically isolated by the 1- $\mu$ m MPM diaphragm. DNase and RNase treatments were done on the EB stained *E. coli* cells on a glass slide according to the procedures described previously<sup>7</sup>.

The photographs were taken at a magnification of  $\times 625$  on 35-mm Fuji 400 film with a 50-sec exposure time using an Olympus BH epi-fluorescent microscope, which was equipped with a high-pressure mercury vapor lamp HBO 100 W, 545-nm excitation filter (IF 545 + BG 36), a 580-nm dichroic mirror (DM 580 + O 590), a 610-nm barrier filter (R 610) and an UVFL 100/1.30 objective. The exposed films were developed at 20°C for 7 min in Fuji Pandol developer. Negatives of phages were scanned at 620 nm with a Joyce-Loebl MK3C microdensitometer. The light spot, which sited the negative of single phage, projected through an objective of magnification 10 onto a slit of

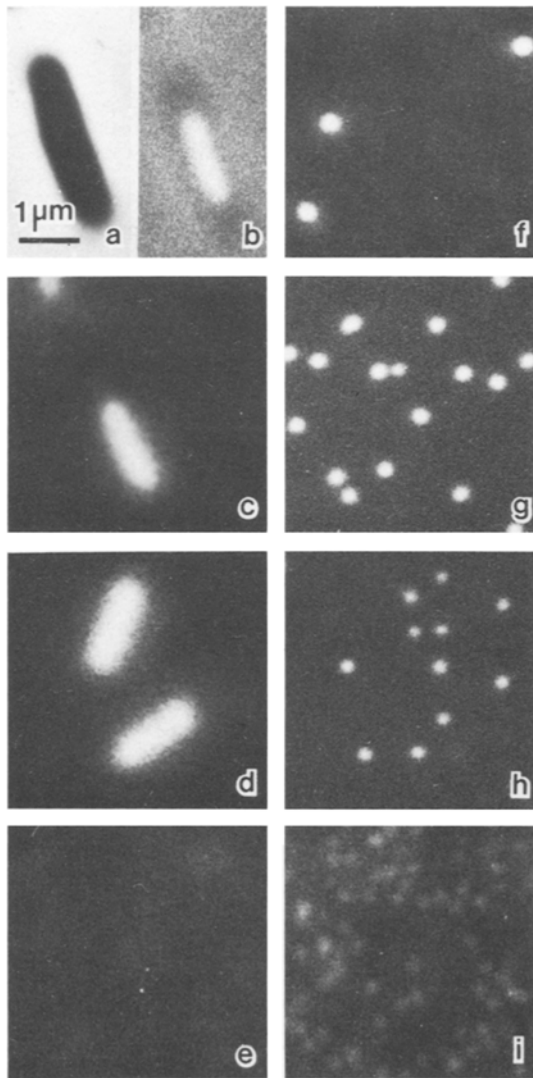


Figure 1. Phase contrast (a), phase contrast-fluorescent (b) and fluorescent micrographs (c-i) illustrating *Escherichia coli* (a-e), T4 phages (f),  $\chi$  phages (g), T7 phages (h) and  $\phi 29$  phages (i) after the EB staining. (a), (b) and (c) are the same field. The fluorescence appeared in the bacterial nuclei but not in the matrix area (a-c). After DNase treatment the fluorescence disappeared completely (e) but after RNase treatment the fluorescence appeared in the bacterial nuclei (d).  $\times 7000$ .

dimensions  $10 \times 0.5$  mm. The density per single phage obtained by one-dimensional scan was integrated with a computer NOVA (Nippon Data General) coupled to the densitometer. More than 100 phage particles were examined in each species.

**Results and discussion.** In *E. coli* cells stained with EB dissolved in distilled water,  $> 60\%$  of the fluorescent intensity was lost within 60 sec after the beginning of illumination with green light. On the other hand, in the cells stained with EB in buffer-NS, the fading was kept within 10% during at least 120 sec. However, when the cells were excited with UV instead of green light,  $> 60\%$  of the fluorescent intensity was lost after 60 sec regardless of the use of buffer-NS. Therefore, the use of 545 nm as the excitation wavelength, EB and buffer-NS may be suitable for observation and fluorometry of a very small amount of DNA.

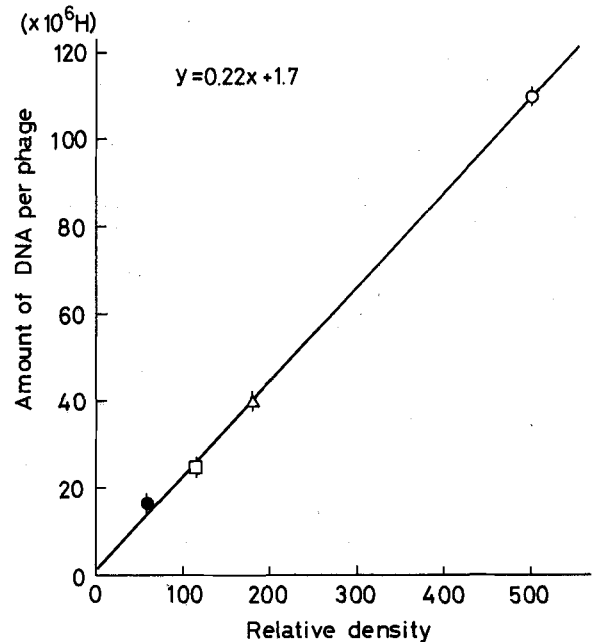


Figure 2. A relationship between relative density of T4 phages ( $\circ$ ),  $\chi$  phages ( $\Delta$ ), T7 phages ( $\square$ ) and  $\phi 29$  phages ( $\bullet$ ) and DNA contents of the phages obtained from biophysical techniques. The formula is  $y = 0.22x + 1.7$ .

Fluorescent intensity of various phages obtained from the densitometry

Phage	No. of phages observed	Relative density*
T4	234	$510 \pm 38$
$\chi$	174	$193 \pm 42$
T7	156	$128 \pm 30$
$\phi 29$	172	$62 \pm 11$

\*Mean values;  $p < 0.05$ .

Figure 1 shows phase contrast (fig. 1a), phase contrast-fluorescent (fig. 1b) and fluorescent micrographs (fig. 1b-i) illustrating *E. coli* (fig. 1a-e), T4 phages (fig. 1f),  $\chi$  phages (fig. 1g), T7 phages (fig. 1h) and  $\phi 29$  phages (fig. 1i) after EB staining. The fluorescence appeared in the bacterial nuclei but not in the matrix (fig. 1a-c). After DNase treatment, the fluorescence in the nuclei disappeared completely (fig. 1e); but after RNase treatment the fluorescence remained (fig. 1d), and their intensity was very similar to that of control cells. The results show that EB specifically stains DNA under the buffer condition. All phages were visualized as the light diffusion areas although their real images could not be observed by the light microscope. Compared with *E. coli*, all phages were remarkably lower in fluorescent intensity. The T4 phages had stronger fluorescence than other phages, while  $\phi 29$  phages could be seen as faint particles. Variation in the fluorescent intensity per particle was small in each species (fig. 1f-i). The table shows fluorescent intensity of T4,  $\chi$ , T7 and  $\phi 29$  phages obtained by the densitometry. Molecular weights of T4,  $\chi$ , T7 and  $\phi 29$  phages are  $110 \times 10^6$  daltons<sup>8</sup>,  $42 \times 10^6$  daltons<sup>9</sup>,  $25 \times 10^6$  daltons<sup>10</sup> and  $11.5 \times 10^6$  daltons<sup>6</sup>, respectively. Therefore, the fluorescent intensity decreased gradually according to diminution of the amount of DNA in each phage. As shown in figure 2, the fluorescent intensity per phage was in proportion to the DNA content in each phage

obtained by biophysical techniques. The relationship could be formularized as  $y = 0.22x + 1.7$ .

The establishment of the EB staining method means that at the level of individual microorganisms or organelles, it is possible to measure a quantity of DNA in organelles such as mitochondria by application of fluorometry.

- 1 Acknowledgments. This work was supported in part by the grant No. 521708 and No. 511212 from the Japan Ministry of Education, Science and Culture.

- 2 D.H. Williamson and D.J. Fennell, in: *Methods in Cell Physiology*, vol. 12, p. 335. Ed. D.M. Prescott. Academic Press, New York 1975.  
 3 T.W. James and C. Jope, *J. Cell Biol.* 79, 623 (1978).  
 4 J.B. Le Pecq and C. Paoletti, *J. molec. Biol.* 27, 87 (1967).  
 5 A. Giese, in: *Cell Physiology*, p. 76. W.B. Saunders Co., Philadelphia 1979.  
 6 E. Anderson and D. Mosharafa, *J. Virol.* 2, 1185 (1968).  
 7 T. Kuroiwa, *J. Cell Biol.* 63, 299 (1974).  
 8 D. Freifelder, *J. molec. Biol.* 54, 567 (1970).  
 9 S.Z. Schade and J. Adler, *J. Virol.* 1, 591 (1967).  
 10 S.B. Leighton and B.I. Rubenstein, *J. molec. Biol.* 46, 313 (1969).

## Presence of double stranded regions of viral RNA in infected cells

S.I. Koliais

*Department of Virology, Theagenion Medical Institute, Thessaloniki (Greece), 11 December 1980*

**Summary.** Ribonuclease treatment of rhinovirus-infected human embryo lung cells after cell disruption reveals that double stranded RNA is present in the preparation before nucleic acids are extracted with phenol. This shows that the hydrogen bonding between complementary molecules of viral RNA which occurs in infected cells is not a result of the extraction of RNA with phenol.

Virus-specific double stranded RNA (DS RNA) has been found so far in cells infected with bacterial, plant and animal viruses which have RNA (single or double stranded) as genetic material. Although it has been suggested that DS RNA plays an active role in the replication of viral RNA<sup>1</sup> many investigators believe that DS RNA does not exist in the infected cell in vivo, but is formed during the extraction of RNA with phenol<sup>2,3</sup>. There is some experimental evidence to support this for RNA phages<sup>4,5</sup>, but there is no definite information in the case of animal RNA viruses. Most RNA viruses are sensitive to the antiviral activity of interferon and this has been shown to be enhanced by DS RNA<sup>6-12</sup>; this is suggestive but not direct evidence for the presence of DS RNA in the infected cell. In this communication we present direct evidence which supports the view that hydrogen bonding between complementary molecules of viral RNA occurs in cells infected with rhinovirus type 2, and that this is not a result of the extraction of RNA with phenol.

We have previously reported the details of the replication of the RNA of rhinovirus type 2 in human embryo lung cells and described the different viral RNA species detectable in this system<sup>13</sup>. Essentially in cells infected with the virus there are 3 RNA species induced which, in order of electrophoretic mobility, are the multi-stranded RNA (MS) which is the replicative intermediate of the replication, double stranded (DS) which is the replicative form, and single stranded RNA (SS), which is identical with the genome of the virus (fig. A). To test whether the replicative form or the replicative intermediate exist in the infected cell in whole or in part in double stranded form, we have tested their sensitivity to RNase in crude extracts prepared by freezing and thawing the cells before the nucleic acids were extracted with phenol.

Details of infection, the extraction of nucleic acids and their analysis by polyacrylamide gel electrophoresis have been described before<sup>13</sup>. In brief,  $50 \times 10^6$  of HEL cells were infected with rhinovirus type 2 and were treated with actinomycin D (1  $\mu\text{g/ml}$ ) for 5-9 h p.i. Since we have previously shown that the viral double stranded RNA is accumulated late in the replication cycle<sup>13</sup> we have labelled with 20  $\mu\text{Ci/ml}$  of [<sup>3</sup>H]-uridine for 9-11 h p.i., and then cells were disrupted by freezing and thawing in  $2 \times \text{SSC}$

(300 mM sodium chloride and 30 mM trisodium citrate, pH 8.45). In the broken cells after treatment with RNase for 10 min at 35 °C with 0.1 or 10  $\mu\text{g/ml}$  of enzyme, SDS was added (1%) and the nucleic acids were extracted with phenol and analyzed by electrophoresis.

If the hydrogen bonding between complementary RNA molecules is formed during the extraction of the RNA with phenol, this treatment of the broken cells with RNase before the extraction should cause degradation of all single stranded RNA molecules. There would therefore be no DS RNA in the fraction of nucleic acids which are subsequently extracted. This, however, should not rule out the possibility that hydrogen bonding could be formed prior to the extraction with phenol, during the disruption of the cells.

The table and the figure show the results of such an experiment using 2 concentrations of RNase. In figure A the positions of the MS, DS and SS RNA in 1.8% polyacrylamide gel are presented. Figures B and C show the electrophoretic pattern of the same cell extract after treatment with 0.1  $\mu\text{g}$  RNase/ml and 10  $\mu\text{g}$  RNase/ml respectively. The table lists the integrated counts in the 3 peaks of viral RNA corresponding to figures A, B and C. It can be clearly seen that treatment with 0.1  $\mu\text{g/ml}$  of RNase eliminates the peak of SS RNA and reduces the peak corresponding to the MS RNA. The amount of DS RNA, however, is not reduced but increased. This is probably because some of the replicative intermediate, after the removal of the single nascent strands, is converted to DS cores which are similar to the replicative form. At a concentration of 10  $\mu\text{g/ml}$  of RNase the SS RNA and the MS RNA are completely degraded but the DS RNA is still present. Finally it should be pointed out that the ribosomal RNA present in the samples was 100% sensitive to both

Treatment with RNase of infected broken cells

RNase ( $\mu\text{g/ml}$ )	MS RNA cpm	%	DS RNA cpm	%	SS RNA cpm	%
0	2560	100	1920	100	9315	100
0.1	1020	40	3060	159	830	8.9
10	45	1.7	2675	140	520	5.5